

# Ionization Structure and the Reverse Shock in E0102-72

K.A. Flanagan, C.R. Canizares, D.S. Davis, D. Dewey, J.C. Houck,  
M.L. Schattenburg

*Center for Space Research, Massachusetts Institute of Technology  
Cambridge, MA 02139*

**Abstract.** The young oxygen-rich supernova remnant E0102-72 in the Small Magellanic Cloud has been observed with the High Energy Transmission Grating Spectrometer of Chandra. The high resolution X-ray spectrum reveals images of the remnant in the light of individual emission lines of oxygen, neon, magnesium and silicon. The peak emission region for hydrogen-like ions lies at larger radial distance from the SNR center than the corresponding helium-like ions, suggesting passage of the ejecta through the "reverse shock". We examine models which test this interpretation, and we discuss the implications.

## BACKGROUND

E0102-72 (hereinafter referred to as E0102-72) is a young ( $\sim 1000$  years) oxygen-rich supernova remnant (SNR) in the Small Magellanic Cloud. E0102-72 has been observed at all wavelengths: in the optical (Dopita *et al.*, 1981; Tuohy and Dopita, 1983), in the UV (Blair *et al.*, 1989; Blair, *et al.*, 2000), in the radio (Amy and Ball, 1993), and in the X-ray (Seward and Mitchell, 1981; Hayashi, *et al.*, 1994; Gaetz *et al.*, 2000; Hughes *et al.*, 2000; Davis *et al.*, 2000; Canizares *et al.*, 2000; Rasmussen, *et al.*, 2000). Gaetz *et al.* have looked at direct *Chandra* images of E0102-72 and noted the radial variation with energy bands centered on OVII and OVIII, suggesting an ionizing shock propagating inward. This paper addresses this issue through analysis of the high resolution dispersed spectrum, and reinforces this interpretation.

## THE HIGH RESOLUTION X-RAY SPECTRUM

Shown below in Figure 1 is the dispersed high resolution X-ray spectrum of E0102-72. The Chandra observation was made using the High Energy Transmission Gratings (HETG) in conjunction with the Advanced CCD Imaging Spectrometer (ACIS-S). The HETG separates the X-rays into their distinct emission lines,

forming separate images of the remnant with the X-ray light of each line. The dispersed spectrum contains lines of highly ionized oxygen, neon, magnesium and silicon (not shown in the figure). Note the distorted shape of the NeX Lyman  $\alpha$  line relative to the zeroth order. This is due to Doppler shifts associated with high velocity material (Houck, *et al.*, 2000.) Note also that there are different radii: these are likely caused by the changing ionization state, suggesting the passage of the supernova ejecta through the reverse shock. This is explored in detail below.

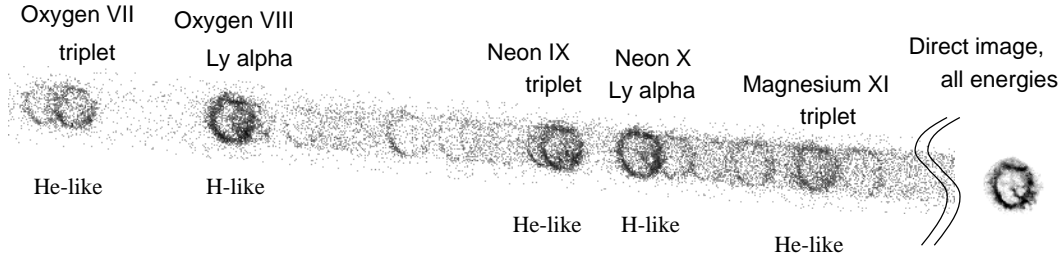


**FIGURE 1.** A portion of the high resolution spectrum formed by the medium energy gratings. At right in the figure is the zeroth order, which combines all energies in an undispersed image.

## THE IONIZATION/SHOCK STRUCTURE OF E0102-72

Figure 2 compares helium-like and hydrogen-like lines of oxygen. The dispersed OVII Resonance line from the helium-like triplet (left) is displayed next to the hydrogen-like OVIII Ly  $\alpha$  line (right) on the same spatial scale. The ring diameter of the hydrogen-like line is obviously larger than that of the helium-like line. The ring diameters of these lines were measured by tracing the distribution in the direction orthogonal to the dispersion axis, as shown in Figure 3. (By taking the distribution in the cross-dispersion direction, the result is largely independent of Doppler shift.) The He-like OVII distribution is nestled cleanly within the OVIII, and is measurably narrower in Figure 3. The ring diameters for all the bright lines were measured

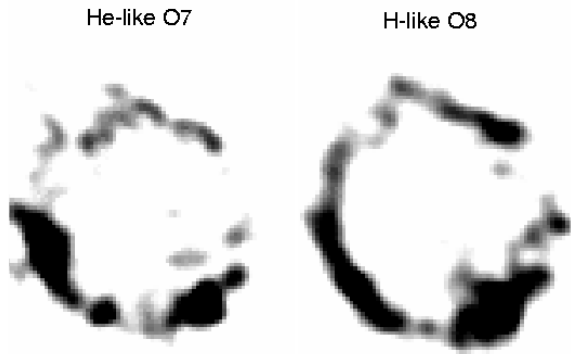


**FIGURE 2.** The OVII Resonance line of oxygen comes from a region of smaller radius than the emitting region of OVIII Lyman  $\alpha$ .

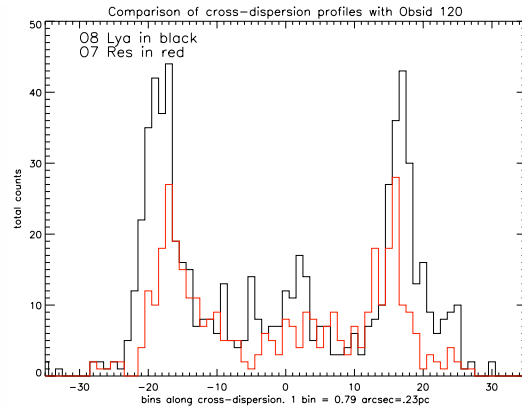


**FIGURE 3.** The helium-like OVII Resonance line distribution is narrower than that of OVIII Lyman  $\alpha$ .

similarly, and the results are shown on Figure 4 (Flanan, *et al.*, 2000). *All of the hydrogen-like lines lie outside the corresponding helium-like lines.*

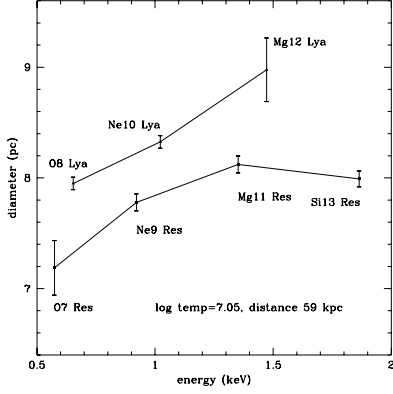


**FIGURE 4.** Ring diameter vs energy for the bright lines. Note that all the hydrogen-like lines (connected by the top curve) lie outside their helium-like counterparts.

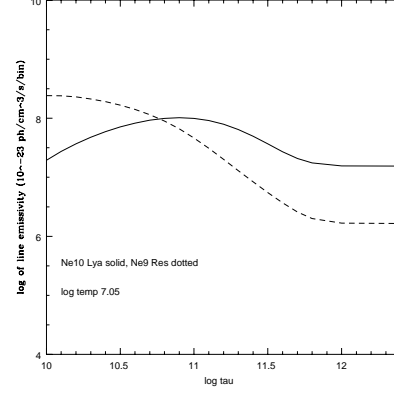


**FIGURE 5.** Helium-like NeIX Resonance line reaches its peak emissivity at  $\log\tau=10.0$ , earlier than hydrogen-like NeX Lyman  $\alpha$ , which peaks at about  $\log \tau=11.0 \text{ sec/cm}^3$

At a fixed electron temperature  $T_e$  and electron density  $n_e$ , a H-like ionization state is created *later* than a He-like state after the passage of a shock. This is shown in Figure 5, where the appropriate timescale is the ionization parameter  $\tau=n_e t$ , where  $t$  is the time since passage of the shock. This suggests the action of a shock moving *inward* relative to the ejecta - the ‘reverse shock’ which is the standard model for the mechanism which heats SNR ejecta to X-ray temperatures. This mechanism is illustrated in Figure 6.

The results of applying a very simple model are shown in the Figure 7. We assume that the ring diameter corresponds to the ionization parameter, estimated by finding the peak emissivity for each bright X-ray line assuming a fixed  $T_e$  of about 1 keV or  $\log T_e=10^{7.05}$  (as suggested by our global NEI analysis). Although any workable model must consider many parameters, the monotonic behavior shown in Figure 7 of the data strongly suggests that these differences in ring diameter are attributable to the ionization structure resulting from the reverse shock.

## WORK IN PROGRESS AND FUTURE WORK

Our current model is very simple and needs further examination. One could consider a plasma in ionization equilibrium at every point, with a radial temperature variation, however our plasma diagnostics consistently indicate a nonequilibrium plasma (Davis, *et al.*, 2000). We may consider taking potentially useful plasma diagnostic line ratios from the cross-dispersion histograms. For example, by taking the ratio of the histograms for O8 Lyman  $\alpha$  and O7 Resonance from Figure 3, we can examine the allowed region of parameter space defined by  $T_e$  and  $\tau$  as a

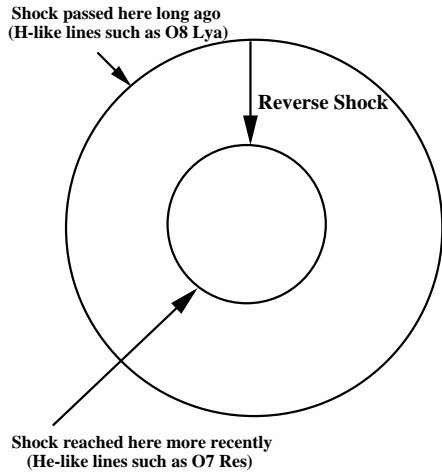


**FIGURE 6.** Reverse shock results in a higher ionization state toward the outside of the remnant.

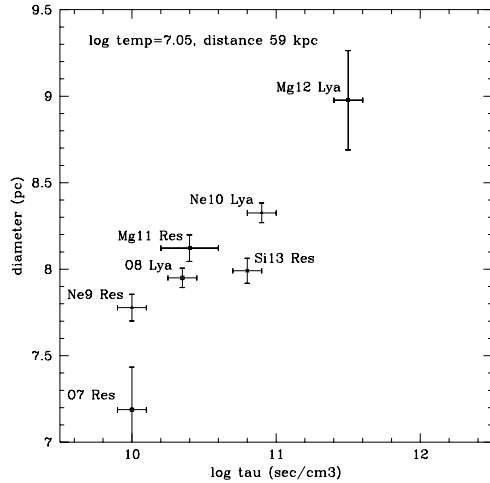


**FIGURE 7.** Measured diameter vs ionization parameter  $\tau$  for the bright lines. As illustrated in Figure 5, the parameter  $\tau$  is that for peak emissivity at the assumed  $T_e$ .

*function of radial position.* If the  $T_e$  can be sufficiently constrained (i.e., to the “asymptotic” region where the ionization age is nearly independent of temperature), then we could examine the ionization structure in detail. Our goal would be to use an appropriate estimate for electron density to obtain a corresponding estimate for the reverse shock velocity, and compare it against the electron temperature. We plan to apply this shock velocity information to see how it fits with the spatial extent of the bright ejecta and the presumed age of the remnant.

## ACKNOWLEDGEMENTS

We thank Glenn Allen, Norbert Schulz and Sara-Anne Taylor for helpful discussions. We are grateful to the CXC group at MIT for their assistance in analysis of the data. This work was prepared under NASA contract NAS8-38249 and SAO SV1-61010.

## REFERENCES

1. Amy, S.W. & Ball, L., *ApJ*, **411**, 761 (1993)
2. Blair, W.P., Raymond, J.C., Danziger, J. & Matteucci, F., *ApJ*, **338**, 812 (1989)
3. Blair, W.P., Morse, J.A., Raymond, J.C., Kirshner, R.P., Hughes, J.P., Dopita, M.A., Sutherland, R.S., Long, K.S. & Winkler, P.F., *ApJ*, **537**, 667 (2000)
4. Canizares, C.R., Flanagan, K.A., Davis, D.S., Dewey, D., & Houck, J.C., *these proceedings*.

5. Davis, D.S., Flanagan, K.A., Houck, J.C., Allen, G.E., Schulz, N.S., Dewey, D., Schattenburg, & M.L., *these proceedings*.
6. Dopita, M.A., Tuohy, I.R. & Mathewson, D.S., 1981, *ApJ*, **248**, L105 (1981)
7. Gaetz, T.J., Butt, Y.M., Edgar, R.J., Eriksen, K.A., Plucinsky, P.P., Schlegel, E.M. & Smith, R.K., *ApJ*, **534**, L47 (2000)
8. Hayashi, I., Koyama, K., Masanobu, O., Miyata, E., Tsunemi, H., Hughes, J.P. & Petre, R., *PASJ*, **46**, L121 (1994)
9. Hughes, J.P. & Helfand, D.J., *ApJ*, **291**, 544 (1985)
10. Hughes, J.P., Rakowski, C.E. & Decourchelle, A. *ApJ*, (2000) in press
11. Tuohy, I.R. & Dopita, M.A., *ApJ*, **268**, L11 (1983)
12. Rasmussen, A. *et al.*, *these proceedings*.
13. Raymond, J.C. & Smith, B.W., *ApJS*, **35**, 419 (1977)
14. Seward, F.D. & Mitchel, M., *ApJ*, **243**, 736 (1981)